Mineralogical Magazine (2023), **87**, 534–541
doi:10.1180/mgm.2023.24

CAMBRIDGE UNIVERSITY PRESS

Article

Mikenewite, the natural analogue of synthetic α-$Mn^{2+}(S^{4+}O_3)\cdot 3H_2O$, a new sulfite mineral from the Ojuela mine, Mapimí, Mexico

Hexiong Yang*, Robert A. Jenkins, James A. McGlasson, Ronald B. Gibbs and Robert T. Downs
Department of Geosciences, University of Arizona, 1040 E. 4th Street, Tucson, AZ, USA

Abstract

A new mineral species, mikenewite (IMA2022-102), ideally $Mn^{2+}(S^{4+}O_3)\cdot 3H_2O$, has been discovered from the San Judas Chimney, Ojuela mine, Mapimí, Durango, Mexico. It occurs as spheres of platy crystals. Associated minerals include goethite, cryptomelane, adamite and lotharmeyerite. Mikenewite is yellowish in transmitted light, transparent with a white streak and vitreous lustre. It is brittle and has a Mohs hardness of 2½–3. Cleavage is perfect on {101}. The measured and calculated densities are 2.48(5) and 2.467 g/cm^3, respectively. Optically, mikenewite is biaxial (+), with $\alpha = 1.606(5)$, $\beta = 1.614(5)$, $\gamma = 1.627(1)$ (white light), 2V(meas.) = 69(3)° and 2V(calc.) = 77°. An electron microprobe analysis yielded an empirical formula (based on 6 O apfu) of $(Mn_{0.86}Zn_{0.12}Fe_{0.04}Ca_{0.02})_{\Sigma 1.04}(S_{0.98}O_3)\cdot 3H_2O$, which can be simplified to $(Mn,Zn,Fe)(SO_3)\cdot 3H_2O$.

Mikenewite is the natural analogue of synthetic α-$Mn^{2+}(S^{4+}O_3)\cdot 3H_2O$, as well as the Mn-analogue of albertiniite, $Fe^{2+}(S^{4+}O_3)\cdot 3H_2O$. It is monoclinic, with space group $P2_1/n$ and unit-cell parameters $a = 6.6390(3)$, $b = 8.8895(4)$, $c = 8.7900(4)$ Å, $\beta = 96.095(2)°$, $V = 515.83(4)$ Å^3 and $Z = 4$. The crystal structure of mikenewite is characterised by each Mn atom coordinated octahedrally by six O atoms, three from different sulfite O atoms and three from H_2O molecules. Each $S^{4+}O_3$ group is bonded to three Mn atoms, resulting in a sheet parallel to (101) with the sheet composition of $Mn^{2+}(S^{4+}O_3)\cdot 3H_2O$. Such sheets, stacked along $[10\bar{1}]$, are joined together by hydrogen bonds, accounting for the perfect cleavage of the mineral. Mikenewite is dimorphous with orthorhombic *Pnma* gravegliaite, as albertiniite is with fleischerite. Its discovery from the Ojuela mine, which is particularly rich in Zn, implies the possibility of finding Zn-bearing sulfites there as well.

Keywords: mikenewite, new mineral, albertiniite, gravegliaite, polymorphs, crystal structure, Raman, Ojuela mine

(Received 2 March 2023; accepted 4 April 2023; Accepted Manuscript published online: 19 April 2023; Associate Editor: Ferdinando Bosi)

Introduction

A new sulfite mineral species, mikenewite, ideally $Mn^{2+}(S^{4+}O_3)\cdot 3H_2O$, was discovered on a specimen collected from the San Judas Chimney, Ojuela mine, Mapimí, Durango, Mexico. It is named in honour of Mr. Michael Edwin New (1943–2022), the owner of 'Top Gem Minerals Inc. of Tucson'. Mike New was a prominent wholesale mineral dealer and specimen miner. In the past half century, he provided the world with a wide variety of mineral specimens from the Ojuela mine where he had permission to mine and export. Mike New's most spectacular find took place in 1981 in the San Judas chimney where fabulous specimens of purple adamite were encountered. Today, many of these specimens are found worldwide in numerous museums and private collections. The type sample of mikenewite is from a specimen mined by Mike New and his miners. Furthermore, Mike New was kind and generously donated many mineral specimens to local schools for students' education, including the University of Arizona. The new mineral and its name (symbol Mnw) have been approved by the Commission on New Minerals, Nomenclature and Classification (CNMNC) of the International Mineralogical Association (IMA2022-102, Yang *et al.*, 2023). The co-type samples have been deposited at the University of Arizona Alfie Norville Gem and Mineral Museum (Catalogue # 22724) and the RRUFF Project (deposition # R210021) (http://rruff.info) (Lafuente *et al.*, 2015).

Sulfite minerals are quite rare in Nature and only 12 minerals contain the $(S^{4+}O_3)^{2-}$ anionic group in the current IMA-approved mineral list at http://cnmnc.units.it/ (Table 1). Interestingly, all of these minerals were described after the 1980s. Sulfites are generally considered as unstable intermediate products of the oxidation process which transforms sulfides into sulfates and special conditions are necessary to preserve them in Nature, accounting for their paucity (Weidenthaler *et al.*, 1993; Vignola *et al.*, 2016). Nevertheless, sulfite materials have been studied extensively because of their high catalytic activity in the oxidation reaction $SO_2 + ½O_2 + H_2O \rightarrow H_2SO_4$, which is of great interest in industrial applications. For example, sulfite-based advanced oxidation processes have been applied for various removals of contaminants and environmental remediations (e.g. Zhou *et al.*, 2022; Ren *et al.*, 2023). Recovery of tellurium and selenium from (Te,Se)-rich materials by alkaline sulfide leaching followed by sodium sulfite precipitation has been developed (e.g. Zhang and Chen, 2014; Guo *et al.*, 2017). Sulfite materials are used widely as antimicrobial agents and antioxidants for food products, beverages and

Corresponding author: Hexiong Yang; Email: hyang@arizona.edu
Cite this article: Yang H., Jenkins R.A., McGlasson J.A., Gibbs R.B. and Downs R.T. (2023) Mikenewite, the natural analogue of synthetic α-$Mn^{2+}(S^{4+}O_3)\cdot 3H_2O$, a new sulfite mineral from the Ojuela mine, Mapimí, Mexico. *Mineralogical Magazine* **87**, 534–541. https://doi.org/10.1180/mgm.2023.24

Table 1. List of IMA approved minerals containing the sulfite anionic group $(S^{4+}O_3)^{2-}$.

Mineral	Ideal chemical formula	Symmetry	Reference
Albertiniite	$Fe^{2+}(SO_3)\cdot 3H_2O$	$P2_1/n$	Vignola *et al.* (2016)
Fleisstalite	$Fe^{2+}(SO_3)\cdot 3H_2O$	*Pnma*	Walter and Bojar (2017)
Mikenewite	$Mn^{2+}(S^{4+}O_3)\cdot 3H_2O$	$P2_1/n$	This study
Gravegliaite	$Mn^{2+}(S^{4+}O_3)\cdot 3H_2O$	*Pnma*	Basso *et al.* (1991)
Scotlandite	$Pb(S^{4+}O_3)$	$P2_1/m$	Paar *et al.* (1984)
Hannebachite	$Ca(SO_3)\cdot \frac{1}{2}H_2O$	*Pbna*	Hentschel *et al.* (1985)
Kollerite	$(NH_4)_2Fe^{3+}(SO_3)_2(OH)\cdot H_2O$	*Cmcm*	Fehér *et al.* (2021)
Orschallite	$Ca_3(S^{4+}O_3)_2(SO_4)\cdot 12H_2O$	$R\bar{3}c$	Weidenthaler *et al.* (1993)
Hielscherite	$Ca_6Si_2[(SO_4)_2(SO_3)_2(OH)_{12}]\cdot 22H_2O$	$P6_3$	Pekov *et al.* (2012)
Steudelite	$Na_3(K_{17}Ca_7)Ca_4(Al_{24}Si_{24}O_{96})(SO_3)_6F_6\cdot 4H_2O$	$P\bar{6}2c$	Chukanov *et al.* (2022)
Tomiolloite	$Al_{12}(Te^{4+}O_3)_5[(SO_3)_{0.5}(SO_4)_{0.5}](OH)_{24}$	$P6_3/m$	Missen *et al.* (2022)
Alloriite	$(Na,K,Ca)_{24}(Na,Ca)_4Ca_4(Si,Al)_{48}O_{96}(SO_4)_4(SO_3,CO_3)_2(OH,Cl)_2(H_2O,OH)_4$	*P*31*c*	Chukanov *et al.* (2007); Rastsvetaeva *et al.* (2007)

pharmaceutical products (Sezgintürk, 2005; Yin *et al.*, 2017; Fehér *et al.*, 2021 and references therein). This paper describes the physical and chemical properties of mikenewite and its crystal structure determined from single-crystal X-ray diffraction data.

Sample description and experimental methods

Occurrence

Mikenewite was found on a specimen (Fig. 1) collected from the San Judas Chimney, Ojuela mine (25°47'36"N, 103°47'27"W), Mapimí, Durango, Mexico. Associated minerals include goethite FeO(OH), cryptomelane $K(Mn_7^{4+}Mn^{3+})O_{16}$, adamite $Zn_2(AsO_4)(OH)$ and lotharmeyerite $CaZn_2(AsO_4)_2\cdot 2H_2O$. A review on the geology and mineralogy of the Ojuela mine has been given by Moore and Megaw (2003), which contains a section of the mining history at the Ojuela mine by Mr. Mike New (pages 47–53), after whom we name the new mineral. The Ojuela mine is the type locality for seven minerals, including lotharmeyerite, $CaZn_2(AsO_4)_2\cdot 2H_2O$ (Dunn, 1983), mapimite, $Zn_2Fe^{3+}{}_3(AsO_4)_3(OH)_4\cdot 10H_2O$ (Cesbron *et al.*, 1981), metaköttigite, $(Zn,Fe^{3+})_3(AsO_4)_2\cdot 8(H_2O,OH)$ (Schmetzer *et al.*, 1982), miguelromeroite, $Mn_5(AsO_3OH)_2(AsO_4)_2(H_2O)_4$ (Kampf, 2009), ojuelaite, $ZnFe_2^{3+}(AsO_4)_2(OH)_2\cdot 4H_2O$ (Cesbron *et al.*, 1981), paradamite, $Zn_2(AsO_4)(OH)$ (Switzer, 1956) and the new mineral mikenewite, described herein.

Physical and chemical properties and Raman spectra

Mikenewite occurs as spheres of platy crystals (Figs 2 and 3) on a matrix of goethite, cryptomelane, adamite and lotharmeyerite.

Figure 1. The specimen on which the new mineral mikenewite was found (Specimen number R210021).

Figure 2. A microscopic view of yellow spheres made of platy mikenewite crystals (Specimen number R210021).

Individual crystals of mikenewite are up to $0.50 \times 0.10 \times 0.04$ mm. Mikenewite is yellowish in transmitted light, transparent with a white streak and vitreous lustre. It is brittle and has a Mohs hardness of 2½–3. Cleavage is perfect on {101}. The density measured by flotation in heavy liquids is 2.48(5) g/cm^3 and the calculated density is 2.467 g/cm^3 based on the empirical chemical formula and unit-cell volume from single-crystal X-ray diffraction data. Optically, mikenewite is biaxial (+), with $\alpha = 1.606(5)$, $\beta = 1.614(5)$, $\gamma = 1.627(1)$ (determined in white light), 2V(meas.) = 69(3)° and

Figure 3. A back-scattered electron image of aggregates (spheres) of platy mikenewite crystals (Specimen number R210021).

https://doi.org/10.1180/mgm.2023.24 Published online by Cambridge University Press

2V(calc.) = 77°. The pleochroism is from grey to yellowish and dispersion is weak, with $r > v$. The calculated Gladstone–Dale compatibility index based on the empirical formula is 0.032 (excellent) (Mandarino, 1981). Mikenewite is insoluble in water, but dissolves slowly in hydrochloric acid.

The chemical composition of mikenewite was determined using a Cameca SX-100 electron microprobe (wavelength dispersive spectroscopy mode, 15 kV, 4 nA and a beam diameter of 20 μm). The standards used for the probe analysis are given in Table 2, along with the determined compositions (7 analysis points). The resultant chemical formula, calculated on the basis of 6 O atoms per formula unit (from the structure determination), is $(Mn_{0.86}Zn_{0.12}Fe_{0.04}Ca_{0.02})_{\Sigma 1.04}(S_{0.98}O_3)\cdot 3H_2O$, which can be simplified to $(Mn,Zn,Fe)(SO_3)\cdot 3H_2O$.

The Raman spectrum of mikenewite was collected on a randomly oriented crystal with a Thermo Almega microRaman system, using a solid-state laser with a wavelength of 532 nm at 75 mW power and a thermoelectric cooled CCD detector. The laser is partially polarised with 4 cm^{-1} resolution and a spot size of 1 μm.

X-ray crystallography

Both the powder and single-crystal X-ray diffraction data for mikenewite were collected on a Bruker APEX2 CCD X-ray diffractometer equipped with graphite-monochromatised Mo*K*α radiation. The measured powder X-ray diffraction data are in Table 3. The unit-cell parameters obtained from the powder X-ray diffraction data using the program by Downs *et al.* (1993) are: $a = 6.640(4)$, $b = 8.878(6)$, $c = 8.789(6)$ Å, $\beta = 96.08(6)°$ and $V = 514.4(4)$ Å^3.

Single-crystal X-ray diffraction data were collected from a $0.06 \times 0.05 \times 0.05$ mm fragment with frame widths of 0.5° in ω and 30 s counting time per frame. All intensity data were corrected for X-ray absorption using the Bruker program *SADABS* (Bruker, 2001). The systematic absences of reflections suggest the unique space group $P2_1/n$. The crystal structure of mikenewite was solved and refined using *SHELX2018* (Sheldrick, 2015a, 2015b). During the structure refinements, the small amount of Ca was ignored and Fe was treated as Mn due to their similar X-ray scattering powers. The refined Mn/Zn ratio at the octahedral site is 0.90/0.10, which is very close to that (0.88/0.12, normalised) measured from the electron microprobe analysis. All H atoms were located through the difference-Fourier syntheses. The positions of all atoms were refined with anisotropic displacement parameters, except for H atoms, which were refined with a fixed isotropic displacement parameter ($U_{iso} = 0.05$). The refinement statistics are given in Table 4. Final atomic coordinates and displacement parameters are given in Tables 5 and 6, respectively. Selected bond distances and the hydrogen bonding scheme are presented in Tables 7 and 8, respectively. The bond-valence sums were calculated using the parameters given by Brown (2009) (Table 9). The crystallographic information file has been deposited with the Principal Editor of *Mineralogical Magazine* and is available as Supplementary material (see below).

Table 2. Analytical chemical data (in wt.%) for mikenewite.

Constituent	Mean	Range	S.D.	Probe standard
MnO	31.75	31.51–32.29	0.29	Rhodochrosite
ZnO	5.25	4.93–5.65	0.22	ZnO (synthetic)
FeO	1.64	1.31–1.85	0.23	Fayalite
CaO	0.56	0.53–0.61	0.03	Anorthite
SO_2	32.54	32.16–33.00	0.30	Baryte
H_2O	28.15			Added in ideal value
Total*	99.89	99.61–101.02	0.57	

* Mikenewite is extremely prone to the electron beam damage. To minimise the damage by the electron beam, we had to lower the current to 4 nA with a beam size of 20 μm. S.D. – standard deviation.

Table 3. Powder X-ray diffraction data (d in Å, I in %) of mikenewite.*

I_{obs}	d_{obs}	I_{cal}	d_{cal}	h	k	l
9	6.228	13	6.228	0	1	1
42	**5.547**	42	5.554	$\bar{1}$	0	1
9	5.298	16	5.293	1	1	0
31	5.006	36	5.014	1	0	1
100	**4.707**	100	4.708	$\bar{1}$	1	1
25	4.433	23	4.439	0	2	0
38	4.367	39	4.370	0	0	2
49	**3.947**	45	3.958	0	2	1
49	**3.924**	46	3.921	0	1	2
22	3.683	20	3.682	1	2	0
60	**3.327**	68	3.324	1	2	1
16	3.236	21	3.237	1	1	2
45	**3.097**	51	3.090	2	1	0
33	3.013	46	3.009	$\bar{2}$	1	1
28	2.905	36	2.902	$\bar{1}$	2	2
57	**2.774**	53	2.776	$\bar{1}$	0	3
32	2.649	31	2.646	2	2	0
23	2.596	23	2.595	$\bar{2}$	2	1
14	2.551	18	2.549	1	3	1
20	2.457	19	2.450	0	3	2
8	2.352	5	2.353	$\bar{1}$	2	3
23	2.253	26	2.254	1	3	2
11	2.222	6	2.222	1	2	3
36	2.185	25	2.185	0	0	4
20	2.124	16	2.123	$\bar{3}$	1	1
13	2.080	11	2.080	3	0	1
23	2.022	21	2.030	1	4	1
17	1.952	20	1.960	0	2	4
26	1.883	24	1.883	3	2	1
23	1.876	20	1.874	$\bar{2}$	1	4
6	1.843	10	1.841	2	4	0
11	1.813	17	1.812	$\bar{3}$	1	3
9	1.758	9	1.758	0	3	4
24	1.741	21	1.734	$\bar{2}$	4	2
23	1.703	11	1.702	3	3	1
19	1.690	18	1.691	$\bar{1}$	5	1
10	1.680	6	1.679	1	4	3
4	1.645	6	1.642	3	1	3
17	1.620	17	1.619	2	2	4
6	1.559	8	1.563	2	5	0
9	1.544	9	1.544	1	2	5
5	1.506	4	1.507	$\bar{3}$	4	2
15	1.499	11	1.497	$\bar{1}$	3	5
9	1.453	5	1.455	3	3	3
11	1.447	6	1.449	2	5	2
16	1.437	12	1.440	4	3	0
9	1.385	6	1.388	$\bar{4}$	0	4
10	1.381	4	1.378	$\bar{3}$	5	1
7	1.367	4	1.369	2	4	4
15	1.305	9	1.303	$\bar{2}$	5	4
7	1.272	3	1.271	5	1	1

*The strongest lines are given in bold.

Crystal-structure description and discussion

Mikenewite is the natural analogue of synthetic α-$Mn^{2+}(S^{4+}O_3)\cdot 3H_2O$ (Baggio and Baggio, 1976; Lutz *et al.*, 1977; Engelen and Freiburg, 1979; Johansson and Lindqvist, 1980), as well as the

https://doi.org/10.1180/mgm.2023.24 Published online by Cambridge University Press

Table 4. Comparison of crystallographic data of mikenewite with related minerals.

	Mikenewite (natural)	Mikenewite (synthetic)	Gravegliaite	Albertiniite
Ideal chemical formula	$Mn^{2+}(S^{4+}O_3)\cdot 3H_2O$	$Mn^{2+}(S^{4+}O_3)\cdot 3H_2O$	$Mn^{2+}(S^{4+}O_3)\cdot 3H_2O$	$Fe^{2+}(S^{4+}O_3)\cdot 3H_2O$
Crystal symmetry	Monoclinic	Monoclinic	Orthorhombic	Monoclinic
Space group	$P2_1/n$	$P2_1/n$	*Pnma*	$P2_1/n$
a (Å)	6.6390(3)	6.6501(3)	9.763(1)	6.633(1)
b (Å)	8.8895(4)	8.9065(4)	5.635(1)	8.831(1)
c (Å)	8.7900(4)	8.7925(4)	9.558(1)	8.773(1)
β (°)	96.095(2)	96.105(3)	90	96.106(8)
V (Å^3)	515.83(4)	525.83	525.83	511.0(1)
Z	4	4	4	4
ρ_{cal} (g/cm^3)	2.467	2.425	2.39	-
2θ range for data collection	≤66.32 (Mo *Kα*)	≤70	≤60	≤72.33
No. of reflections collected	7365	2280	1641	14415
No. of independent reflect.	1947		829	1668
No. of reflect. with $I > 2\sigma(I)$	1633	1749	594	1409
No. of parameters refined	92			92
R(int)	0.0277			0.0339
Final R_1, wR_2 factors [$I > 2\sigma(I)$]	0.025, 0.056	0.021	0.036, 0.058	0.023, 0.043
Goodness-of-fit	1.052			1.657
Reference	This study	Engelen and Freiburg (1979)	Basso *et al.* (1991)	Vignola *et al.* (2016)

Table 5. Fractional atomic coordinates and equivalent isotropic displacement parameters (Å^2) for mikenewite.

Atom	*x/a*	*y/b*	*z/c*	U_{iso}*/U_{eq}
Mn**	0.43086(3)	0.24689(2)	0.64354(3)	0.01284(7)
Zn**	0.43086(3)	0.24689(2)	0.64354(3)	0.01284(7)
S	0.67451(5)	0.57024(4)	0.67378(4)	0.01300(10)
O1	0.54450(17)	0.69750(13)	0.59497(13)	0.0190(2)
O2	0.77740(17)	0.64257(13)	0.81998(13)	0.0207(3)
O3	0.52070(17)	0.46359(12)	0.73310(14)	0.0182(2)
O4	0.11068(18)	0.34728(14)	0.64347(15)	0.0190(2)
O5	0.2641(2)	0.04567(15)	0.57326(16)	0.0269(3)
O6	0.36377(19)	0.16726(14)	0.87396(14)	0.0191(2)
H1	0.058(4)	0.326(3)	0.700(3)	0.050*
H2	0.113(4)	0.455(3)	0.646(3)	0.050*
H3	0.255(4)	0.010(3)	0.493(3)	0.050*
H4	0.165(4)	0.025(3)	0.622(3)	0.050*
H5	0.246(5)	0.175(3)	0.895(3)	0.050*
H6	0.453(4)	0.178(3)	0.956(3)	0.050*

** Occupancies: Mn = 0.904(7); Zn = 0.096(7)

Table 7. Selected bond distances (Å) for mikenewite and gravegliaite.

	Natural mikenewite (monoclinic)	Synthetic mikenewite (orthorhombic)	Gravegliaite (monoclinic)
Mn–O1	2.1770(12)	2.178(2)	2.162(4)
Mn–O2	2.1406(11)	2.151(2)	2.173(3) × 2
Mn–O3	2.1416(11)	2.149(2)	2.187(4)
Mn–O4	2.3054(12)	2.314(2)	2.255(3) × 2
Mn–O5	2.1590(13)	2.242(2)	
Mn–O6	2.2346(12)	2.169(2)	
<Mn–O>	2.1930	2.200	2.201
OAV*	38.21	39.72	22.16
OQE*	1.012	1.012	1.007
S–O1	1.5420(12)	1.544(2)	1.535(4)
S–O2	1.5313(11)	1.529(2)	1.531(3) × 2
S–O3	1.5252(12)	1.529(2)	
<S–O>	1.5239	1.535	1.532
Reference:	This study	Engelen and Freiburg (1979)	Basso *et al.* (1991)

*OAV – octahedral angle variance and OQE – octahedral quadratic elongation (Robinson *et al.*, 1971).

Mn-analogue of albertiniite, $Fe^{2+}(S^{4+}O_3)\cdot 3H_2O$ (Johansson and Lindqvist, 1979; Vignola *et al.*, 2016). It is noteworthy that, in addition to monoclinic $P2_1/n$ mikenewite and albertiniite, both $Mn^{2+}(S^{4+}O_3)\cdot 3H_2O$ and $Fe^{2+}(S^{4+}O_3)\cdot 3H_2O$ possess an orthorhombic *Pnma* polymorph, namely, gravegliaite (Baggio and Baggio, 1976; Basso *et al.*, 1991; Gonschorek *et al.*, 1996; Diaz de Vivar *et al.*, 2006) and fleisstalite (Walter and Bojar, 2017).

The crystal structure of mikenewite is characterised by each Mn atom coordinated by six O atoms, three from different sulfite O atoms and three from H_2O molecules, giving rise to a slightly distorted octahedron (Table 7). Each $S^{4+}O_3$ group is bonded to three Mn atoms, resulting in a sheet parallel to (101) with the sheet composition of $Mn^{2+}(S^{4+}O_3)\cdot 3H_2O$ (Fig. 4). Such sheets, stacked along [10$\bar{1}$], are joined together by hydrogen bonds

Table 6. Atomic displacement parameters (Å^2) for mikenewite.

Atom	U^{11}	U^{22}	U^{33}	U^{12}	U^{13}	U^{23}
Mn	0.01303(11)	0.01269(11)	0.01270(12)	0.00019(7)	0.00096(8)	0.00186(8)
S	0.01103(16)	0.01513(17)	0.01297(18)	−0.00014(12)	0.00186(12)	0.00039(13)
O1	0.0192(5)	0.0216(5)	0.0164(6)	0.0037(4)	0.0030(4)	0.0070(5)
O2	0.0181(5)	0.0273(6)	0.0158(6)	−0.0091(4)	−0.0016(4)	−0.0005(5)
O3	0.0198(5)	0.0139(5)	0.0215(6)	−0.0044(4)	0.0056(4)	−0.0002(4)
O4	0.0183(5)	0.0184(5)	0.0204(6)	0.0002(4)	0.0029(4)	0.0016(5)
O5	0.0357(7)	0.0277(6)	0.0188(6)	−0.0133(5)	0.0101(5)	−0.0084(5)
O6	0.0153(5)	0.0279(6)	0.0140(5)	0.0010(4)	0.0016(4)	0.0021(4)

https://doi.org/10.1180/mgm.2023.24 Published online by Cambridge University Press

Table 8. Hydrogen-bond geometry (Å, °) in mikenewite (*D* = donor, *A* = acceptor).

D—H···*A*	*D*—H	H···*A*	*D*···*A*	*D*—H···*A*
O4—H1···O1^{iv}	0.66(3)	2.30(3)	2.9365(18)	162(3)
O4—H2···O6^{v}	0.96(3)	1.91(3)	2.8546(17)	172(2)
O5—H3···O2^{vi}	0.77(3)	2.06(3)	2.7940(17)	161(3)
O5—H4···O3^{iv}	0.85(3)	1.94(3)	2.7729(19)	168(3)
O6—H5···O1^{iv}	0.83(3)	1.95(3)	2.7660(17)	170(3)
O6—H6···O4^{vii}	0.89(3)	1.87(3)	2.7370(17)	165(3)

Symmetry codes: (iv): $-x + ½, y - ½, -z + 3/2$; (v) $-x + ½, y + ½, -z + 3/2$; (vi) $x - ½, -y + ½, z - ½$; (vii) $x + ½, -y + ½, z + ½$.

Table 9. Bond-valence sums for mikenewite.

	Mn	S	Σ
O1	0.344	1.317	1.661
O2	0.380	1.356	1.736
O3	0.379	1.379	1.758
O4	0.243		0.243
O5	0.361		0.361
O6	0.295		0.295
Σ	2.002	4.052	

(Fig. 5), accounting for the perfect cleavage of the mineral. In comparison, the crystal structure of gravegliaite consists of chains formed by MnO_6 octahedra and $S^{4+}O_3$ groups, which run parallel to [010] and are linked together by hydrogen bonds (Baggio and Baggio, 1976; Basso *et al.*, 1991; Diaz de Vivar *et al.*, 2006). Although Mn^{2+} cations in mikenewite and gravegliaite have a similar coordination environment ($3O^{2-} + 3H_2O$), the MnO_6 octahedron in mikenewite appears to be noticeably more distorted than that in gravegliaite in terms of both OAV (octahedral angle variance) and OQE (octahedral quadratic elongation) (Robinson *et al.*, 1971) (Table 7).

The Raman spectrum of mikenewite is plotted in Fig. 6, along with that of isostructural albertiniite, $Fe^{2+}(S^{4+}O_3)\cdot 3H_2O$ (Vignola *et al.*, 2016) for comparison. The strong resemblance between the two spectra is evident. Based on the Raman spectroscopic study on albertiniite (Vignola *et al.*, 2016), we made the following tentative assignments of major Raman bands for mikenewite. The broad bands (relatively strong) centred at 3219 and 3365 cm^{-1} and those (very weak) between 1500 and 1700 cm^{-1} are due to the O–H stretching and H–O–H bending modes in H_2O groups, respectively. The bands between 730 and 1080 cm^{-1} are ascribable to the S^{4+}–O stretching vibrations within the $S^{4+}O_3$ groups, whereas those from 430 to 700 cm^{-1} originate from the O–S^{4+}–O bending modes. The bands below 380 cm^{-1} are associated mainly with the rotational and translational modes of $S^{4+}O_3$ groups, as well as the (Mn^{2+})–O interactions and lattice vibrational modes.

The calculated bond-valence sums for mikenewite (Table 9) indicate that all three O atoms (O1, O2 and O3) in the sulfite $S^{4+}O_3$ group are noticeably under-bonded (1.66, 1.74 and 1.76 valence units, respectively). Their deficiencies in bond-valence sums are compensated by H bonds, as all these O atoms are engaged in the hydrogen bonding as acceptors (Table 8). In particular, O1 is the acceptor for two H bonds (O4–H1···O1 = 2.937 Å and

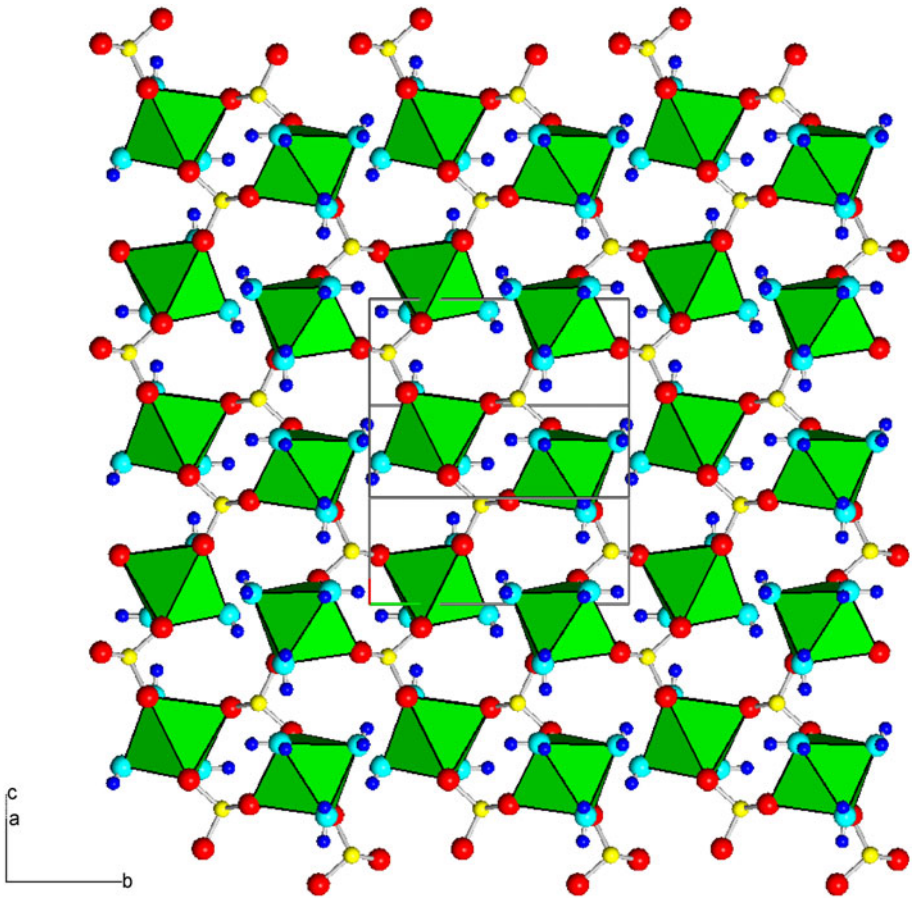

Figure 4. Crystal structure of mikenewite, showing a sheet [‖(101)] consisting of $[MnO_3(H_2O)_3]$ octahedra (green) connected by $(S^{4+}O_3)^{2-}$ groups. Red, aqua, yellow and small blue spheres represent O from $(S^{4+}O_3)^{2-}$, O from H_2O, S and H atoms, respectively. Drawn using *XtalDraw* (Downs and Hall-Wallace, 2003).

https://doi.org/10.1180/mgm.2023.24 Published online by Cambridge University Press

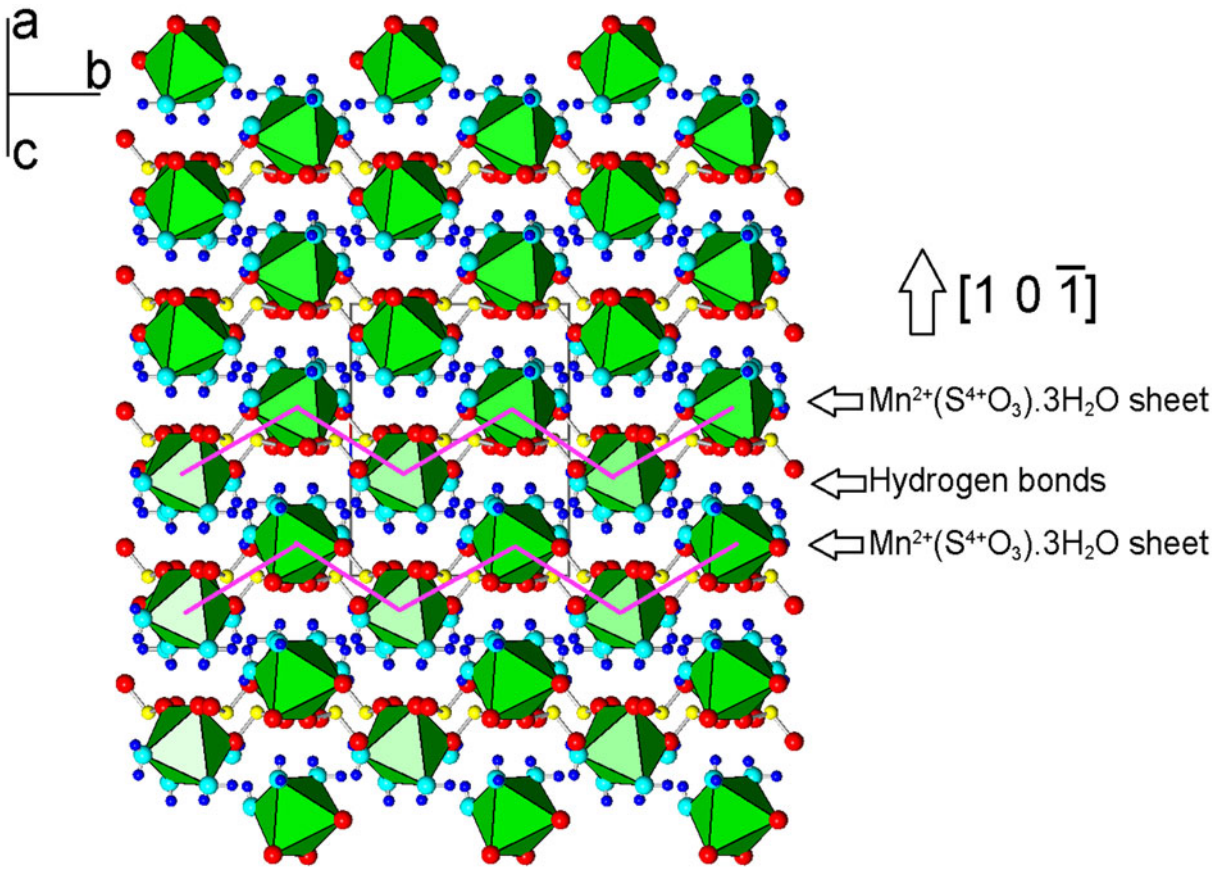

Figure 5. Crystal structure of mikenewite, showing the stacking of sheets consisting of $[MnO_3(H_2O)_3]$ octahedra (green) connected by $(S^{4+}O_3)^{2-}$ groups. Two sheets are specifically indicated by the zigzag purple lines. These sheets are stacked along [1 0 $\bar{1}$] and are linked together by hydrogen bonds. Drawn using *XtalDraw* (Downs and Hall-Wallace, 2003). The legends are the same as in Fig. 4.

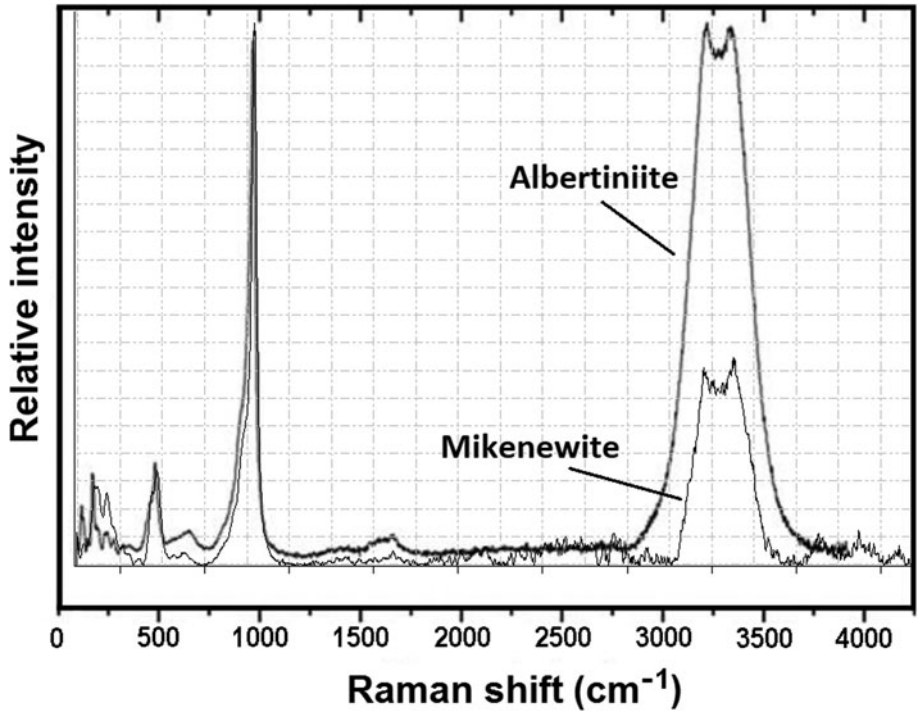

Figure 6. Raman spectrum of mikenewite, along with that of albertiniite (taken from Vignola *et al.*, 2016) for comparison.

https://doi.org/10.1180/mgm.2023.24 Published online by Cambridge University Press

O6–H5···O1 = 2.766 Å). According to the correlation between O–H stretching frequencies (cm^{-1}) and O—H···O distances (Å) for minerals (Libowitzky, 1999), the Raman bands between 3200 and 3380 cm^{-1} we observed for mikenewite correspond well with the O–O distances between 2.73 and 2.94 Å (Table 8).

In addition to Mn^{2+}- and Fe^{2+}-sulfite trihydrates, a number of hydrous M^{2+}-sulfite compounds (M = Mg, Zn, Co, Ca, Cu, etc) have also been synthesised, including several Zn sulfites, such as $ZnSO_3{\cdot}2½H_2O$, $ZnSO_3{\cdot}2H_2O$, $ZnSO_3{\cdot}½H_2O$ and $ZnSO_3$ (e.g. Lutz *et al.*, 1977; Inoue *et al.*, 1999; Lagosz and Malolepszy, 2003; Giorgi *et al.*, 2011). Because the Ojuela mine is particularly rich in Zn, as exemplified by numerous Zn-bearing minerals, typically adamite and lotharmeyerite (Moore and Megaw, 2003), one may postulate, based on the discovery of mikenewite, the possibility of finding Zn-bearing sulfites there. The fact that the mikenewite we examined in this study contains 12% Zn substituting for Mn lends good support to this conjecture.

Acknowledgements. The constructive comments by Drs. Peter Leverett, Pietro Vignola and Oleg Vereshchagin are greatly appreciated. This study was funded by the Feinglos family and Mr. Michael M. Scott.

Supplementary material. The supplementary material for this article can be found at https://doi.org/10.1180/mgm.2023.24.

Competing interests. The authors declare none.

References

Baggio R.F. and Baggio S. (1976) Crystal structure and chemical bonding of manganese(II) sulphite trihydrate. *Acta Crystallographica*, **B32**, 1959–1962.

Basso R., Lecchetti G and Palenzona A. (1991) Gravegliaite, $MnSO_3{\cdot}3H_2O$, a new mineral from Val Graveglia (Northern Apennines, Italy). *Zeitschrift für Kristallographie*, **197**, 97–106.

Brown I.D. (2009) Recent developments in the methods and applications of the bond valence model. *Chemical Reviews* **109**, 6858–6919.

Bruker (2001) *SADABS*. Bruker AXS Inc., Madison, Wisconsin, USA.

Cesbron F., Romero M. and Williams S. (1981) La mapimite et l'ojélaïte, deux nauveaux arséniates hydratés de zinc et de fer de la mine Ojuela, Mapimi, Mexique. *Bulletin de Minéralogie*, **104**, 582–586.

Chukanov N.V., Rastsvetaeva R.K., Pekov I.V. and Zadov AE (2007) Alloriite, $Na_5K_{1.5}Ca(Si_6Al_6O_{24})(SO_4){\cdot}(OH)_{0.5}{\cdot}H_2O$, a new mineral of the cancrinite group. *Zapiski Rossiiskogo Mineralogicheskogo Obshchetstva*, **136**, 82–89.

Chukanov N.V., Zubkova N.V., Varlamov D.A., Pekov I.V., Belakovskiy D.I., Britvin S.N., Van K.V., Ermolaeva V.N., Vozchikova S.A. and Pushcharovsky D.Y. (2022) Steudelite, $(Na_3\square)[(K, Na)_{17}Ca_7]Ca_4(Al_{24}Si_{24}O_{96})(SO_3)_6F_6{\cdot}4H_2O$, a new cancrinite-group mineral with afghanite-type framework topology. *Physics and Chemistry of Minerals*, **49**, 1–12.

Diaz de Vivar M.E., Baggio S., Garland M.T. and Baggio R. (2006) Triaquamanganese sulfite revisited. *Acta Crystallographica*, **C62**, i79–i82.

Downs R.T. and Hall-Wallace M. (2003) The American Mineralogist Crystal Structure Database. *American Mineralogist*, **88**, 247–250.

Downs R.T., Bartelmehs K.L., Gibbs G.V. and Boisen M.B., Jr (1993) Interactive software for calculating and displaying X-ray or neutron powder diffractometer patterns of crystalline materials. *American Mineralogist*, **78**, 1104–1107.

Dunn P.J. (1983) Lotharmeyerite, a new mineral from Mapimi, Durango, Mexico. *The Mineralogical Record*, **14**, 35–36.

Engelen B. and Freiburg C. (1979) Kristallstruktur von Mangan(II) sulfit-trihydrat α- $MnSO_3(H_2O)_3$. *Zeitschrift für Naturforschung*, **B34**, 1495–1499.

Fehér B., Sajó I., Kótai L., Szakáll S., Ende M., Effenberger H., Mihály J., Szabó D. and Koller G. (2021) Three new ammonium-iron-sulfite phases from a burning dump of the vasas abandoned opencast coal mine, Pécs, Mecsek Mts., Hungary. *Acta MineralogicaPetrographica*, **11**, 11 [abstracts].

Giorgi G., Lyutov G.L. and Lyutov L.G. (2011) Single-crystals of magnesium sulfite hexahydrate doped with nickel–structure, density and optical properties. *Bulgarian Chemical Communications*, **43**, 236–243.

Gonschorek W., Weitzel H. and Engelen B. (1996) Neutron diffraction study of β– $MnSO_3{\cdot}3D_2O$ anharmonic motion of oxygen and hydrogen, statistical tests of intensity variances, refinement including weak and negative intensities. *Zeitschrift für Kristallographie-Crystalline Materials*, **211**, 674–678.

Guo X., Xu Z., Li D., Tian Q., Xu R. and Zhang Z. (2017) Recovery of tellurium from high tellurium-bearing materials by alkaline sulfide leaching followed by sodium sulfite precipitation. *Hydrometallurgy*, **171**, 355–361.

Hentschel G., Tillmanns E. and Hofmeister W. (1985) Hannebachite, natural calciumsulfite hemihydrite, $CaSO_3{\cdot}½H_2O$. *Neues Jahrbuch für Mineralogie, Monatshefte*, **1985**, 241–250.

Inoue M., Grijalva H., Inoue M. B. and Fernando Q. (1999) Spectroscopic and magnetic properties of Chevreul's salt, a mixed valence copper sulfite $Cu_3(SO_3)_2{\cdot}2H_2O$. *Inorganica Chimica Acta*, **295**, 125–127.

Johansson L.G. and Lindqvist O. (1979) The crystal structure of iron(II) sulfite trihydrate, α-$FeSO_3.3H_2O$. *Acta Crystallographica*, **B35**, 1017–1020.

Johansson L.G. and Lindqvist O. (1980) Manganese(II) sulfite trihydrate. *Acta Crystallographica*, **B36**, 2739–2741.

Kampf A.R. (2009) Miguelromeroite, the Mn analogue of sainfeldite, and redefinition of villyaellenite as an ordered intermediate in the sainfeldite-miguelromeroite series. *American Mineralogist*, **94**, 1535–1540.

Lafuente B., Downs R.T., Yang H. and Stone N. (2015) The power of databases: the RRUFF project. Pp. 1–30 in: *Highlights in Mineralogical Crystallography* (T Armbruster and R M Danisi, editors). W. De Gruyter, Berlin, Germany.

Lagosz A. and Malolepszy J. (2003) Tricalcium aluminate hydration in the presence of calcium sulfite hemihydrate. *Cement and Concrete Research*, **33**, 333–339.

Lutz H.D., El-Suradi S. and Engelev B. (1977) Zur Kenntnis der Sulfite und Sulfithydrate der Zink-, Mangan-, Magnesium- und Cobalt-rontgenographischen, Spektroskopischen und Thermoanalytischen Untersuchungen. *Zeitschrift für Naturforschung*, **B32**, 1230–1238.

Mandarino J.A. (1981) The Gladstone–Dale relationship. IV. The compatibility concept and its application. *The Canadian Mineralogist*, **19**, 441–450.

Missen O.P., Mills S.J., Rumsey M.S., Spratt J., Najorka J., Kampf A.R. and Thorne B. (2022) The new mineral tomiolloite, $Al_{12}(Te^{4+}O_3)_5[(SO_3)_{0.5}(SO_4)_{0.5}](OH)_{24}$: A unique microporous tellurite structure. *American Mineralogist*, **107**, 2167–2175.

Moore T.P. and Megaw P.K.M. (2003) Famous mineral localities: The Ojuela mine, Mapimi, Durango, Mexico. *The Mineralogical Record*, **34**, 1–91.

Paar W.H., Braithwaite R.S.W., Chen T.T. and Keller P. (1984) A new mineral, scotlandite ($PbSO_3$) from Leadhills, Scotland; the first naturally occurring sulphite. *Mineralogical Magazine*, **48**, 283–288.

Pekov I.V., Chukanov N.V., Britvin S.N., Kabalov Y.K., Göttlicher J., Yapaskurt V.O., Zadov A.E., Krivovichev S.V., Schüller W. and Ternes B. (2012) The sulfite anion in ettringite-group minerals: a new mineral species hielscherite, $Ca_3Si(OH)_6(SO_4)(SO_3){\cdot}11H_2O$, and the thaumasite-hielscherite solid-solution series. *Mineralogical Magazine*, **76**, 1133–1152.

Rastsvetaeva R.K., Ivanova A.G., Chukanov N.V. and Verin I.A. (2007) Crystal structure of alloriite. *Doklady Earth Sciences*, **415**, 815–819.

Ren Y., Chu Y., Li N., Lai B., Zhang W., Liu C. and Li J. (2023) A critical review of environmental remediation via iron-mediated sulfite advanced oxidation processes. *Chemical Engineering Journal*, **455**, 140859.

Robinson K., Gibbs G.V. and Ribbe P.H. (1971) Quadratic elongation: A quantitative measure of distortion in coordination polyhedra. *Science*, **172**, 567–570.

Schmetzer K., Amthauer G., Stähle V. and Medenbach O. (1982) Metaköttigit, $(Zn,Fe^{3+})(Zn,Fe^{3+},Fe^{2+})_2(AsO_4)_2{\cdot}8(H_2O,OH)$, ein neues Mineral aus Mapimi, Mexiko. *Neues Jahrbuch für Mineralogie, Monatshefte*, **1982**, 506–518.

Sezgintürk M.K. and Dinçkaya E. (2005) Direct determination of sulfite in food samples by a biosensor based on plant tissue homogenate. *Talanta*, **65**, 998–1002.

Sheldrick G.M. (2015a) SHELXT – Integrated space-group and crystal structure determination. *Acta Crystallographica*, **A71**, 3–8.

Sheldrick G.M. (2015b) Crystal structure refinement with SHELX. *Acta Crystallographica*, **C71**, 3–8.

Switzer G. (1956) Paradamite, a new zinc arsenate from Mexico. *Science*, **123**, 1039- 1039.

Vignola P., Gatta G.D., Rotiroti N., Gentile P., Hatert F., Baijot M., Bersani D., Risplendente A. and Pavese A. (2016) Albertiniite, $Fe^{2+}(SO_3)\cdot 3H_2O$, a new sulfite mineral species from the Monte Falò Pb-Zn mine, Coiromonte, Armeno Municipality, Verbano Cusio Ossola Province, Piedmont, Italy. *Mineralogical Magazine*, **80**, 985–994.

Walter F. and Bojar H.-P. (2017) Fleisstalite, $Fe^{2+}(SO_3)\cdot 3H_2O$, a new sulfite mineral species. *Mitteilungen der Österreichischen Mineralogischen Gesellschaft*, **163**, 92–92.

Weidenthaler C., Tillmanns E. and Hentschel G. (1993) Orschallite, $Ca_3(SO_3)_2(SO_4)\cdot 12H_2O$, a new calcium-sulfite-sulfate-hydrate mineral. *Mineralogy and Petrology*, **48**, 167–177.

Yang H., Jenkins R.A., McGlasson J.A., Gibbs R.B. and Downs R.T. (2023) Mikenewite, IMA 2022-102. CNMNC Newsletter 71; *Mineralogical Magazine*, **87**, https://doi.org/10.1180/mgm.2023.11

Yin C., Li X., Yue Y., Chao J., Zhang Y. and Huo F. (2017) A new fluorescent material and its application in sulfite and bisulfite bioimaging. *Sensors and Actuators B: Chemical*, **246**, 615–622.

Zheng Y.J. and Chen K.K. (2014) Leaching kinetics of selenium from selenium– tellurium-rich materials in sodium sulfite solutions. *Transactions of Nonferrous Metals Society of China*, **24**, 536–543.

Zhou Z., Huang J., Zeng G., Yang R., Xu Z., Zhou Z. and Lyu S. (2022). Insights into the removal of organic contaminants by calcium sulfite activation with Fe (III): Performance, kinetics, and mechanisms. *Water Research*, **221**, 118792.

https://doi.org/10.1180/mgm.2023.24 Published online by Cambridge University Press